

Paper Template for 13th International Conference on Fracture

Yina F. M. Moscoso¹, Anderson S. Barbosa², João B. Uchôa³, Luciano M. Bezerra⁴,
Marcus Sa⁵

^{1,2,3,4,5} Departamento de Tecnologia, Universidade de Brasília, Cep: 70910-900, Brasil
Electronic account: yifemuno@gmail.com

Abstract

Ceramic coatings are generally used on the facades of buildings. These materials provide acoustic and thermal insulation, achieving a reasonable comfort in buildings. The coatings are run in layers: plaster, adhesive mortar, grout and ceramic. They are subject to different weather and thus prompted the actions coming from sudden temperature variation or thermal shock. When you combine these actions with different physical and mechanical characteristics of the materials used, states of stress and strain on the facades are produced, creating different pathologies, such as peeling parts, which can cause accidents on pedestrians. This paper presents a methodology for evaluating the fatigue resistance, using experimental, analytical and numerical analysis via Finite Elements and considering the system under the action of heat loss shock temperature characteristic in the city of Brasília. Studies are in particular the influence of thermo mechanical stresses in fatigue failure of the adhesive mortar. Experimentally a Wöhler curve (or "SN" curve) is obtained for the adhesive mortar. With the appropriate models for fragile materials, the fatigue strength of the mortar under compressive and tensile-compression is deduced. With the values of temperatures and correspondent stresses obtained via analytical and numerical analysis it is possible, with this methodology, to assess the fatigue resistance of the adhesive mortar on the coating system.

Keywords: Fatigue coating, Coatings system, Stress facades

1. Introduction

Coatings on facades of buildings are used, among other purposes, for protection against the weather which have aggressive agents that reduce its lifespan. They also, have the property to give thermal and acoustic comfort to the user inside the building. Thus, the facades are exposed to various situations of thermal loads, arising from changes in temperature and isolation, which results in thermal stresses requested by the materials that make up the coating.

A ceramic coating system is an element for presenting different materials in different applications that must always maintain a balance between the stresses acting on the system and tension resistance of the materials so as not to compromise the integrity of the facade. In this paper we present the stresses inside the structure produced by outside thermal shock, when using clear ceramic (low energetic absorption of heat) and dark ceramic (high-energetic absorption of heat), evaluating the structure performance against thermal shock cycles, which cause fatigue. The fatigue is evaluated by tracing the experimental curve or Wöhler SN, based on the principle that the thermal stresses acting on the system tend to cause their rupture by fatigue and using a coating structure composed of ceramic pieces and grout constituting the outermost layer, connected with a thin layer of adhesive mortar in turn connected to a base composed of plaster. These structures are superposed on a masonry wall, which is coated with a layer of plaster facing the inside of the building. We tried to represent such a constructive disposition commonly used in Brazil.

2. Fatigue

The degradation process by fatigue is linked to deterioration under cyclic loading which leads to the emergence and development of microcracks or microfissures on the pre-existing material, and may cause rupture of the structure. The higher the stress level used, the lower the number of cycles achieved, and thus more rapidly deteriorate the mortar by fatigue, for the same frequency of loading. Coating systems are subject to an increase of stress due to temperature differences between the top and bottom of the wall and the coating system, causing large thermal differential that origin the warpage of the coating.

For the static fatigue analysis breakthrough curves are usually used that can be adapted to cyclic loading. In the analysis of fatigue strength material such as mortar which is a brittle material a classical curve that may be used is the Mohr-Coulomb curve. This curve defines the fatigue resistance of the material and the expected life of the material can be used with the stresses generated by the thermal shock on the system, and indicate whether there is a risk of collapse due to fatigue mortar.

3. Characterization of mortar

In this work the mortar ACII Votomassa was used, prepared according to the manufacturer's recommendations.

3.1. Definition of the body-of-evidence

Fatigue tests in compression, body-of-proof cylindrical 10x20cm were chosen according to the study by SUELEN, 2009.

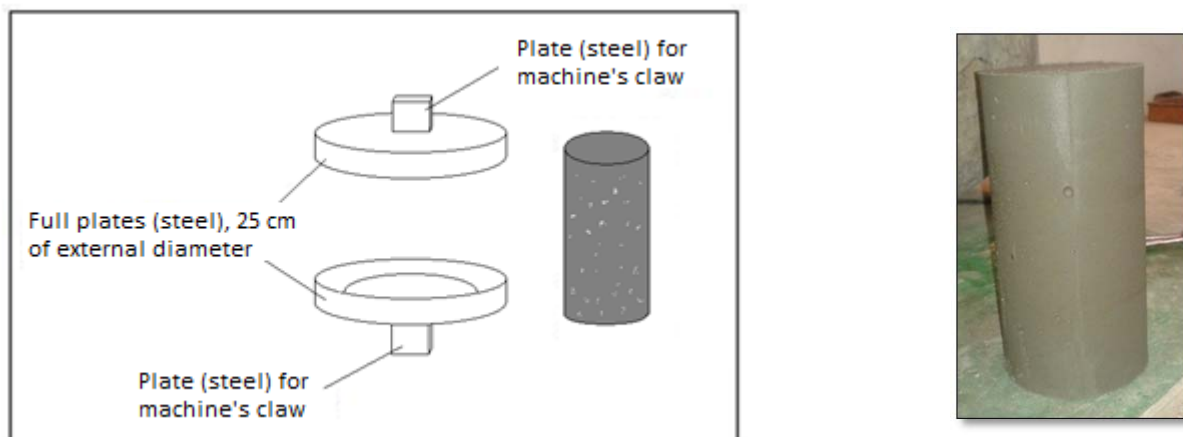


Figure 1 - Mechanism to support the fatigue test and compression test specimen.

3.2 Fatigue Testing

The fatigue test consists in applying a cyclic compression load on a body-of-evidence in order to measure how many cycles the body-of-evidence resists before rupturing. Thus, we obtain the Wöhler curve or SN curve. This assay is also capable of supplying a characteristic alternated stress for each material, below which the body of the test piece no longer breaks. The main results of this assay are: Narrow fatigue resistance (σ_{RF}), ie the alternating stress value below which the body of

the test piece not further ruptures by fatigue; Life fatigue (N_f), or the number of cycles that rupture occurs in the body of the test piece for a particular alternated stress level (S) above (σ_{Rf}).

After sizing the body-of-evidence, the realization of the mortar compression fatigue test is next. The tests were performed on a universal testing machine MTS 810, being made via control force which results in constant amplitude alternating stress across the tests.

The body of the test piece was cast in a mold iron, running in three layers of 4 cm each, and applying 25 blows on each layer. The procedure for determining the body-of-evidence to the MTS 810 was given as follows: initially, for the specimen used in the compression test, we used two circular steel plates holding the specimen fixed. As can be seen in Figure 2a and Figure 2b.

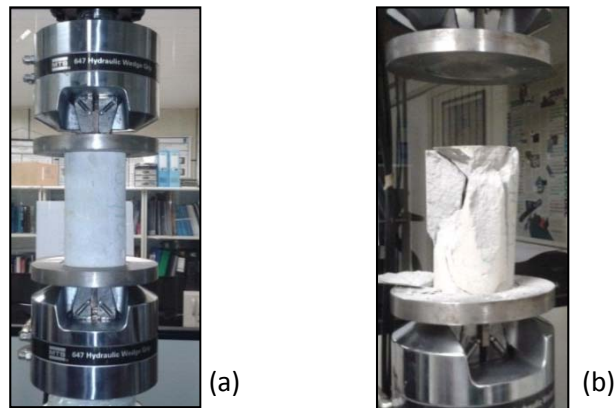


Figure 2– (a) - (b)Endurance test compression.

4. Thermal Analysis

The purpose of the thermal analysis was to determine how the temperature distribution behaves inside the wall, and therefore inside coating structure, after the incidence of atmospheric thermal shock abroad. The first mathematical simplification was made to adopt an equivalent wall composed of only one material, which replaces the conventional wall, composed of five layers of materials. Thus it was possible to work with only one equivalent thermal diffusivity parameter (α_{eq}). The temperature distribution analytical equation $U(y, t)$ varies in function of the wall thickness (direction y) and time (t). It was obtained from the problem depicted in partial differential equation of heat diffusion:

$$\alpha_{eq} \frac{\partial^2 U}{\partial y^2} = \frac{\partial U}{\partial t} \quad (3)$$

The boundary conditions of the problem, then, represent the heat exchanges by conduction and convection at the faces facing the interior and exterior of the building:

$$-K_{eq} \frac{\partial U(d, t)}{\partial y} = h_e (U(d, t) - U_\infty(t)) - \gamma I_g(t) \quad (4)$$

$$-K_{eq} \frac{\partial U(0, t)}{\partial y} = h_i (U_i - U(0, t)) \quad (5)$$

Where $U_\infty(t)$ is the air temperature outside the building, and $I_g(t)$ represents the supply of thermal energy from the sun to the facade over time, modeling it as a source of heat within the system. Having in mind that τ is the time instant at which occurs the heat shock, these features were modeled as it follows:

$$U_{\infty}(t) = U_a + (U_c - U_a)H(t - \tau) \quad (6)$$

$$I_g(t) = \gamma I_g(1 - H(t - \tau)) \quad (7)$$

Where, $H(t - \tau)$ is the Heaviside mathematical function (step function) defined by

$$H(t - \tau) = \begin{cases} 0, & t < \tau \\ 1, & t \geq \tau \end{cases} \quad (8)$$

Other variables of the problem are:

- $K_{eq} = 1,19 \text{ W/m}^\circ\text{C}$: Thermal Conductivity of the equivalent wall;
- $\alpha_{eq} = 6,33 \times 10^{-7} \text{ m}^2/\text{seg}$: Equivalent Thermal diffusivity. Single value of thermal diffusivity for the entire coating structure;
- $d = 25,15 \text{ cm}$: Total thickness of the wall where the structure of ceramic coating, outward looking;
- $l_1 = 2 \text{ cm}$: Thickness of plaster layer facing the interior of the building. Not part of the structure of the ceramic coating;
- $l_2 = 20 \text{ cm}$: Thickness of the masonry wall layer. Substrate where the ceramic coating structure is applied;
- $h_i = 9 \text{ W/m}^2 \text{ }^\circ\text{C}$: Coefficient of air heat transfer from inside the building into the wall structure where the internal plaster layer lays;
- $h_e = 18 \text{ W/m}^2 \text{ }^\circ\text{C}$: Coefficient of atmospheric air heat transfer from outside the building into the wall structure where the ceramic coating lays;
- $U_i = 21^\circ\text{C}$: air temperature inside the building where is the wall subjected to thermal shock;
- $U_a = 34,60^\circ\text{C}$: Temperature of the atmospheric air outside the building moments immediately prior to the occurrence of thermal shock;
- $U_c = 22,14^\circ\text{C}$: Temperature of the atmospheric air outside the building moments immediately following the occurrence of thermal shock;
- λ_n : : Eigenvalues obtained numerically by the following equation:

$$\lambda \cos \lambda d - \frac{\lambda^2 K_{eq}}{h_i} \sin \lambda d + \frac{h_e}{K_{eq}} \sin \lambda d + \frac{\lambda h_e}{h_i} \cos \lambda d = 0 \quad (9)$$

- CF_n : Coefficients of Fourier Series describing the temperature distribution;
- γ : Coefficient of Solar Radiation Absorption of ceramic coating. Worth 0.45 to 0.95 for clear and dark ceramic pottery.
- $I_g = 692 \text{ W/m}^2$: Solar Thermal Energy Incident on the ceramic surface, moments immediately prior to heat shock.

The values of the parameters described were obtained in Saraiva (1998), Moaveni (2008), Uchôa (2007) and Rosa (2001). Thus the modeled thermal shock itself contains a mathematical simplification, which consists in the instant change of atmospheric conditions in contact with the

outer face of the wall. A further simplification is the admission that before the heat shock event, the wall is in a steady state temperature distribution, simplification considered conservative.

Thus, solving the problem has been that the coating structure in equation ($t \geq 0$) is given by:

$$U(y, t) = \frac{h_e U_c K_{eq} + h_i U_i K_{eq} + h_i h_e U_i d + [h_e h_i (U_c - U_i)](y + l_1 + l_2)}{K_{eq}(h_e + h_i) + d h_e h_i} - \sum_{n=1}^{\infty} C F_n e^{-\alpha_{eq} \lambda_n^2 t} \left(\sin \lambda_n (y + l_1 + l_2) + \frac{\lambda_n K_{eq}}{h_i} \cos \lambda_n (y + l_1 + l_2) \right) \quad (10)$$

$$C F_n = \frac{2 \lambda_n^{-1} h_i [h_i^2 (\sin \lambda_n d - \lambda_n d \cos \lambda_n d) + \lambda_n^2 K_{eq} \sin \lambda_n d (h_i d + K_{eq})] [h_e (U_c - U_a) - \gamma l_g]}{(2 \lambda_n K_{eq} h_i (\sin^2 \lambda_n d) + (\lambda_n^2 K_{eq}^2 - h_i^2) \sin \lambda_n d \cos \lambda_n d + \lambda_n d (\lambda_n^2 K_{eq}^2 + h_i^2)) (K_{eq} (h_e + h_i) + d h_e h_i)} \quad (11)$$

Therefore, we obtain values of temperature in each wall layer in the form of one-dimensional distribution.

5. Adopted numerical model

To evaluate the stresses that arise in the three outer layers of the wall (which characterize the structure of the coating) regarding the temperature distribution described by the analytical equation obtained, we choose to model the coating structure with a finite element mesh. Modeling in a coating system of 4.90 m length in each direction, having in mind that Fiorito (1994) suggests that, on a wall, positioning the drive joints should be at least every 4.90 m distance. However, as been done in previous studies of Uchôa (2007) and Saraiva (1998), it is appropriate to focus the analysis in only a small region of that piece of facade. Therefore, a region containing only three ceramic riding up a region equivalent shell around the three ceramics is chosen, as shown in Figure 3 below:

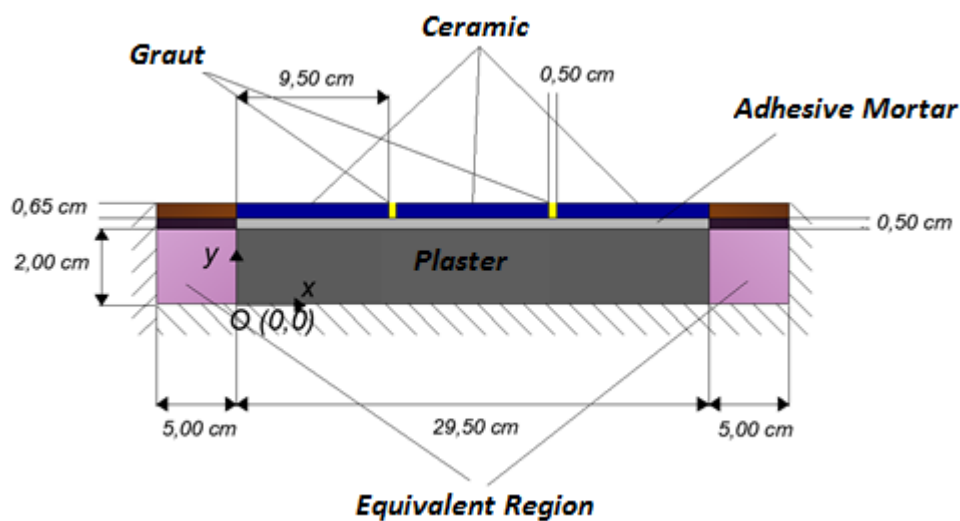


Figure 3-Structure model to be analyzed and dimensions.

The boundary condition used to simulate the structure is based in the assumption that the substrate is rigid. Thus, in the boundary between the coating and the substrate the displacements in the y-axis must be equal to zero. The equivalent regions and their very neighborhood are not considered objects of study, being focus the central regions of the system. The idea would be to avoid disturbances generated at the boundary, which does not produce consistent results, as argued by Saraiva (1998).

Table 1- Material properties of the coating structure and facade equivalent.

Material	Elasticity Modulus - E (GPa)	Thermal Expansion Coefficient - α ($^{\circ}\text{C}^{-1}$)	Poisson's Ratio - ν
Plaster	5,499	$11,5 \times 10^{-6}$	0,2
Mortar	3,562	$8,7 \times 10^{-6}$	0,2
Graut	7,879	$4,2 \times 10^{-6}$	0,2
Ceramic	41,600	$6,8 \times 10^{-6}$	0,2
Eq.Plaster	0,11941	530×10^{-6}	0,2
Eq.Mortar	0,07735	400×10^{-6}	0,2
Eq.Ceramic and Graut	0,78891	310×10^{-6}	0,2

Once modeled of the facade, the application ANSYS (1994) is ran to convert it into finite elements. Among the factors contained in the library of ANSYS (1994) the element named PLANE42 was used, which has four nodes having two degrees of freedom per node: the displacements in the directions "x" and "y". The PLANE42 element accepts temperature as charging, and allows inputting parameters such as elasticity modulus, thermal expansion coefficient of, Poisson's ratio in the materials and structures modeled with the element.

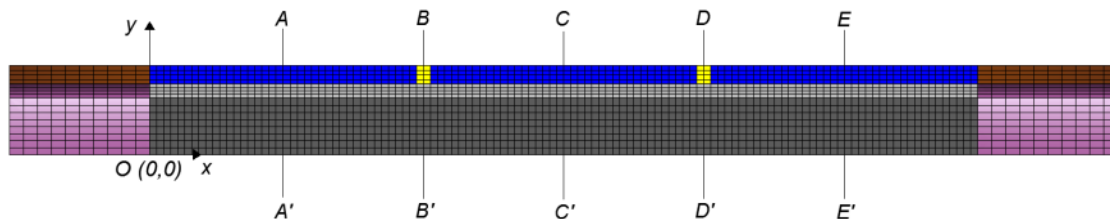


Figure 4 - Finite element mesh structure characterizing the coating studied.

6. Results Presentation

After inserting nodal temperatures in each nodal layer the model, obtained through the temperature distribution equation, the application ANSYS (1994) is ran again, outputting the stresses that affect the coating structure. The stresses obtained were: SX to the normal stresses in the x direction; SY to the normal stress in the y direction; SXY for the shear stresses; and S1 and S2 to the principal stresses.

According to the above, two constructive situations were studied: using clear ceramic, and using dark ceramic. In each case were evaluated three sections shown in Figure 4: AA', passing through

the center of the first ceramic; BB' passing through the layer of grout, and CC' passing through the ceramic core. Therefore, the influence of ceramic and cross-sectional analysis were evaluated.

6.1 Temperature Distribution

As explained in the item 4, we adopted the simplifying assumption that, before the heat shock, the coating structure presented steady state temperature distribution. Therefore the most critical condition in which the structure has higher temperatures is the initial. When the thermal shock atmospheric occurred, the coating structure begins to gradually lose heat to the air, seeking new situation of steady state, with higher speed of temperature decrease in the first few minutes. The clear ceramic shows lower temperatures than the dark because it has a lower coefficient of thermal absorption.

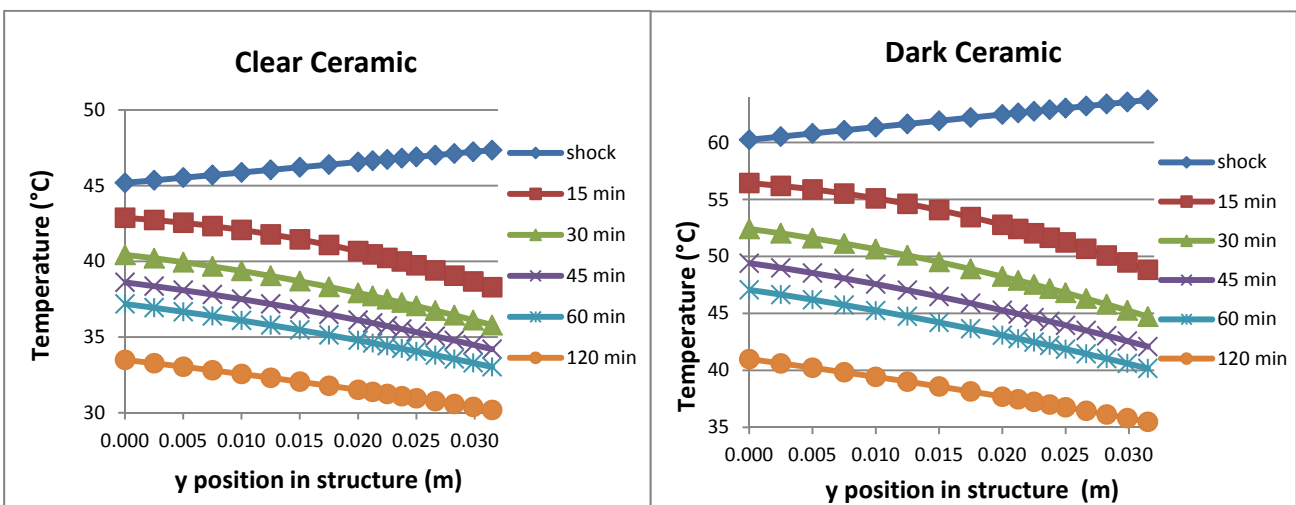


Figure 5 – Temperatures obtained for ceramics dark and clear

6.2 Analysis of stresses

Considering that the highest temperatures are shown at the beginning, also the highest stresses are present at that moment. Because the model with clear ceramic works with lower temperatures, stresses values in this model were lower when compared with the dark ceramic. During the cooling of the layers of the structure, due to thermal shock, there is also the relief of the stresses that request it. Negative values indicate compressive stresses, and the positive tensile stresses.

With regard to stresses SX, it was found that the models worked with compressive stresses in all three layers. This is due to the fact that when the structure is heated before heat shock, it tends to swell; however, their deformation is prevented by the boundary conditions of zero displacement at the ends. From here the compressive stress analysis are originated. The ceramic pieces in sections AA' and CC' have the highest stress values because they have the higher modulus of elasticity (41.6 GPa). Because of high modulus of elasticity, the ceramic ultimately absorb much of the compressive stress that would be passed on to lower layers. Moreover, the grout at BB' top is significantly less rigid than the ceramic (modulus of 7.879 MPa) and therefore ends up being compressed by the ceramic part, deforming and allowing major deformations, thus, allowing the passage of more stresses for the subsequent layers of adhesive mortar and plaster, which is why

tensions SX in plaster and adhesive mortar of BB' section are higher than observed in sections AA' and BB'.

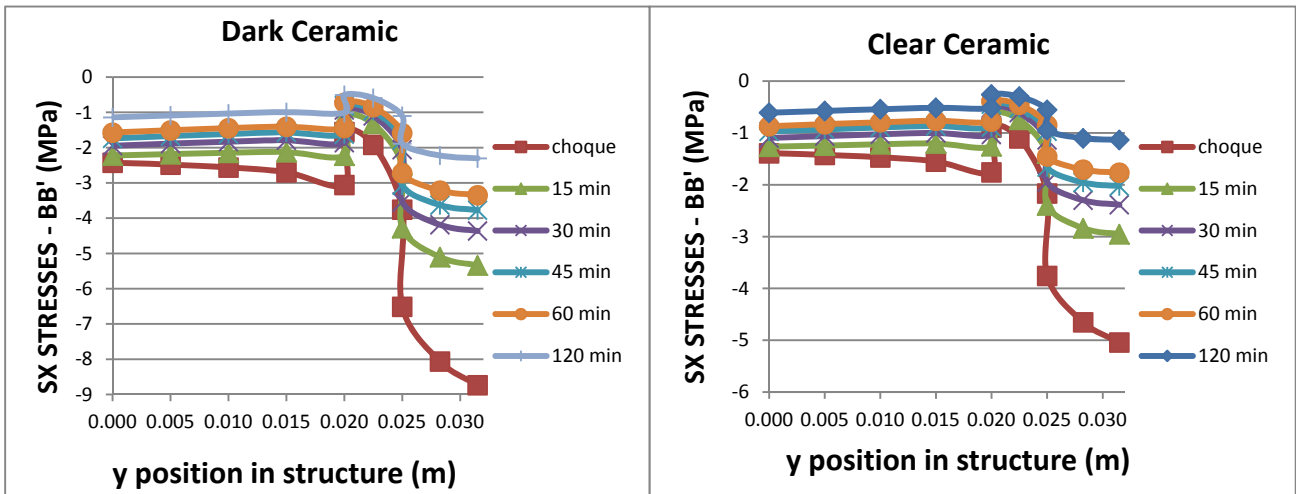


Figure 6 – SX stresses in section BB' after thermal shock, ceramics clear and dark

Regarding the SY stresses, due to the compressive stress in the x direction, the sections AA' and CC' there were tensile stresses in the sense tendency to detachment between layers of the structure. The highest stress values were observed in these layers beneath the layer of plaster, where was restriction of no movement. Moreover, layers of plaster and adhesive mortar section BB' worked with SY compression stresses, and the main reason is because the ceramic parts are compressing the grout in the x direction. In response, crushed grout spreads up and down in the vertical direction, compressing both the adhesive mortar as the plaster situated below it.

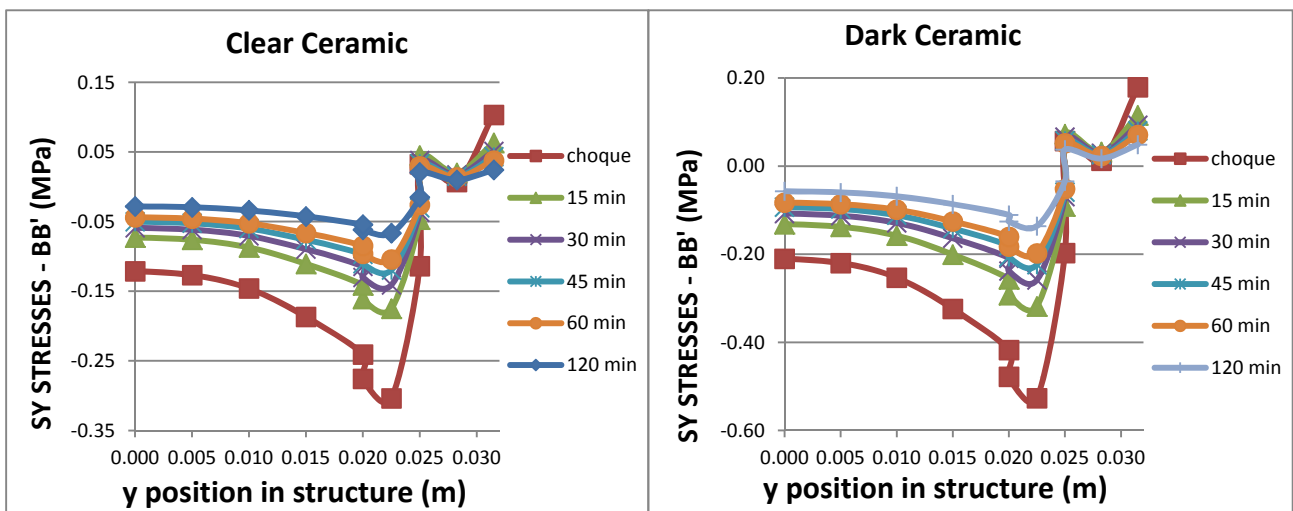


Figure 7 – SY stresses in section BB' after thermal shock, ceramics clear and dark.

The SXY shear stresses encountered to the coating structure in both models were very low compared to the stresses SX and SY. In section CC' the values were effectively zero, due to the central position of this section. The reason for the low values of SXY is because of the deformations within the structure are of thermal nature, which normally do not produce shear stresses. As a result, the values should be more restrictions on movement imposed on the structure than the thermal loading

properly. So, it follows that the principal stresses S1 and S2 have almost the same values SY and SX, respectively.

6.3 Performance of the mortar layer on the fatigue

Given that the thermal shock is a transient phenomenon, which produces variation in the stress state along time, one can understand the difference between the final state and the initial state of stresses as the alternated loads that affect the structure. Then it is appropriate to evaluate the performance of the structure (specifically the adhesive mortar) as fatigue, determining how many cycles of alternating stresses (S) are necessary to the rupture.

In this paper, only the performance of the layer of adhesive mortar is evaluated. For this, Equations 12 and 13 are used, which displays the linearized equation of SN curve (or Wöhler curve) for the adhesive mortar, obtained under test. The critical situations, where the highest stresses occurred, in the mortar, were on top of layer (grout interface) to the stresses S2, and at the base of the layer (plaster interface) to stress S1, both in section BB' section.

$$S = 9,5771 - 0,7523 \log(N), \quad N < 1,1 \times 10^6 \quad (12)$$

$$S = \sigma_{Rf} = 5,06 \text{ MPa}, \quad N > 1,1 \times 10^6 \quad (13)$$

Table 3 – Calculation of alternated stress

CASE1 (CLEAR CERAMIC)			
	PRINCIPAL STRESSES (MPa)		ALTERNATED STRESSES(MPa)
	during shock	120 min	$\Delta S = S (120 \text{ min}) - S (\text{Shock})$
S1	-0,27579	-0,06181	$-0,06181 - (-0,27579) = 0,21398$
S2	-2,16630	-0,55252	$-0,55252 - (-2,16630) = 1,61378$
CASE2 (DARK CERAMIC)			
	PRINCIPAL STRESSES (MPa)		ALTERNATED STRESSES(MPa)
	during shock	120 min	$\Delta S = S (120 \text{ min}) - S (\text{Shock})$
S1	-0,47798	-0,12571	$-0,12571 - (-0,47798) = 0,35227$
S2	-3,75780	-1,10190	$-1,10190 - (-3,75780) = 2,65590$

So for both cases, there is no risk of fatigue failure in any of the directions of principal stress, because the variation of both principal stresses $\Delta S1$ and $\Delta S2$ is smaller than the threshold fatigue resistance ($\sigma_{Rf} = 5,06 \text{ MPa}$).

7. Final Thoughts

The methodology consisted of three phases: characterization tests of the behavior of the adhesive mortar when subjected to cyclic loading; the conception of an analytical equation to explain the temperature distribution inside the coating structure, in response to the incidence of heat loss shock;

and using numerical model in finite elements to determine the stresses arising within the coating due to the temperature distribution over time.

In step test was determined the 5,06Mpa value as the limit of fatigue resistance of the adhesive mortar. In consequence, as the alternated stresses levels in the mortar layer does not reach this value, according to this methodology there is no risk of breakage of this layer to either case. This is due to the fact that among the materials that compose the structure, the mortar is the one with the lowest value of elasticity modulus.

However, it is recommended to apply the methodology also for the other layers, especially layers of grout (subjected to large compression caused by the movement of ceramics) and ceramic (because they are subject to the higher stress levels, including bending stresses). Consequently, it is necessary to perform characterization tests for types of grout, besides testing flexural behavior for ceramic pieces.

References

ANSYS. Analysis System. Houston, PA: ANSYS, 1994. 5.4v.

FIORITO, A. J. S. I. Manual de Argamassas e Revestimentos – Estudos e Procedimentos de Execução”, Editora Pini. São Paulo, SP, 1994

MOAVENI, Finite Element Analysis, Theory and Application with ANSYS. Prentice Hall Inc.. New Jersey, United States, 2008

ROSA, J. A. Determinação dos Campos de Velocidade e Temperatura em Ambientes Ventilados, Dissertação de Mestrado apresentada à Universidade Federal do Rio Grande do Sul, Porto Alegre, RS, 2001

SARAIVA, A. G. Contribuição ao Estudo de Tensões de Natureza Térmica em Sistemas de Revestimento Cerâmico de Fachada. Dissertação de Mestrado apresentada à Faculdade de Tecnologia da Universidade de Brasília, Brasília, DF. 1998.

UCHÔA, J. C. B. Procedimento numérico e experimental para a avaliação da resistência à fadiga de sistemas de revestimento, Dissertação de Mestrado apresentada à Faculdade de Tecnologia da Universidade de Brasília, Brasília, DF, 2007.